

Global Performance Analysis of a Novel Indoor Air Carbon Capture System

Yongting Shen* and Hongxing Yang

Renewable Energy Research Group (RERG), Research Institute for Smart Energy (RISE), The Hong Kong Polytechnic University, Hong Kong, China

ABSTRACT

A global performance analysis with weather conditions from 20 cities is conducted on a solar-driven indoor air carbon capture model to uncover the influence of solar irradiance and ambient temperature on the novel system's carbon capture performance and cooling energy-saving performance. Results show that solar irradiance significantly affects collected CO₂ mass while temperature affects energy-saving amounts. Specifically, for a 40 m² × 2.8 m room with 39 occupants, the proposed system can capture 37.2-41.03 kg CO₂ per day and achieves an energy-saving performance between 23.95%-50.66% in different cities. This study sheds light on effectively and renewably capturing CO₂ from indoor air worldwide.

Keywords: Global performance analysis, Indoor air carbon capture, CO₂ emission reduction, Energy-saving, Solar energy

NOMENCLATURE

Abbreviations	
ICC	Indoor CO ₂ concentration
DAC	Direct air carbon capture
ETC	Evacuated thermal collector
Symbols	
m_{CO_2}	Collected CO ₂ mass (kg)
$p_{CO_2}(t)$	Indoor CO ₂ partial pressure (Pa)
β	Cooling energy-saving (%)

1. INTRODUCTION

Indoor CO₂ concentration (ICC) can be 2-7 times higher than the outside because humans spend 90% of their time indoors [1-4], especially in crowded rooms without proper ventilation. A high ICC potentially causes health issues to occupants[5-13]. Conventional

methods to decrease indoor CO₂ concentration are usually achieved via natural/mechanical ventilation methods that fall short of carbon reduction demands and the pervasiveness of application scenarios.

A growing interest in indoor air carbon capture has arisen recently. Kim. M et al. [14] have investigated implementing a CO₂ adsorption device in an air ventilation system to recirculate indoor air and save 30%-60% ventilation energy. Similarly, Baus et al. [15] have compared the overall energy-saving performance for various environments. Harrouz et al. [16] adopted different adsorbents to remove excess water and CO₂ from the indoors and reported the optimal working conditions for various months. Wang et al. [17] have focused on carbon capture performance and achieved a capacity of 128.4 mg_CO₂ / g_adsorbent, with a regeneration efficiency of 66.7%. Nevertheless, current research fails to provide a complete performance analysis that includes carbon capture and energy-saving performance at the same time. More importantly, both performances are highly sensitive to ambient conditions and have mutual effects on each other, which haven't been properly studied.

Thus, this paper conducts a global performance analysis on a time-dependent solar-driven hybrid indoor air carbon capture model that considers real-time air recirculation. The average summer weather conditions (solar irradiance, ambient temperature, relative humidity) of 20 cities worldwide are adopted to investigate their effects on the proposed system's carbon capture performance and cooling-energy saving performance.

This is a paper for the 14th International Conference on Applied Energy - ICAE2022, Aug. 8-11, 2022, Bochum, Germany.

2. STRUCTURE AND METHODOLOGY

2.1 Proposed scheme

Fig. 1 presents the entire hybrid system scheme, which composes three major parts: a simulated room, a two-chamber adsorption-based carbon capture (CCA) device, and evacuated solar thermal collectors with a buffer tank. The given room size here is $40 \text{ m}^2 \times 2.8 \text{ m}$ with 39 occupants (39.2 kg CO_2 exhaled in 24 hours). Notably, ETCs are located on the rooftop and share the same room area. The useful heat gained is first stored in a buffer tank, from which the hot water flows through the capture chamber and heat adsorbent to the acceptable regeneration temperature $T_{reg}(t)$ to activate the desorption process (chamber 2 when $i=1$ or chamber 1 when $i=3$). The stale air caused by human metabolism acts as the feed gas of the chamber that is

undergoing the adsorption process (chamber 1 when $i=1$ or chamber 2 when $i=3$) when CO_2 is selected and captured by the adsorbent (zeolite 13 X). The other gases that are not captured flow through an electronic valve, which is programmed only to pass “ideal gas” (gases with lower temperature-concentration values than the outside) back to the room ($j=1$), and only pass “not ideal gas” to the outside environment ($j=2$). When CCA undergoes mode 2, valve V2 is turned off, and the two-chamber exchange residual heat with each other. The continuous $\dot{m}_{air}^{i,j,new}$ from the outside ensures a plausible indoor oxygen level. This research adopts the historical average weather conditions from 20 cities worldwide as the inputs to uncover the influence of climate conditions on the system’s capture and energy-saving performance.

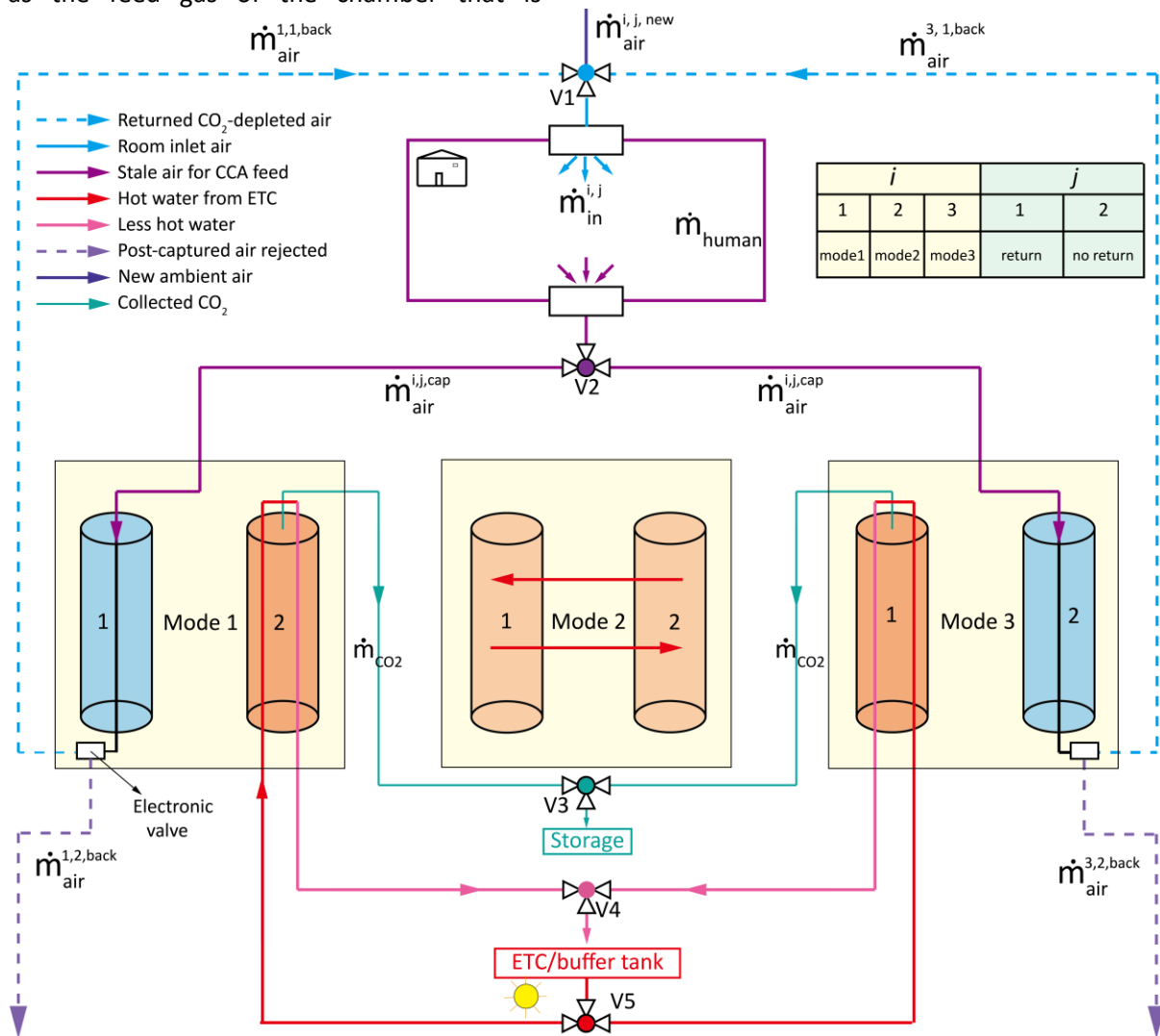


Fig. 1 The overall scheme of the proposed solar-driven indoor air carbon capture hybrid system

2.2 Theory and Calculations

$$T_{reg}(t) = T_{reg}(t-1) + \frac{(Q_w(t) - Q_{reg}(t-1))}{m_{tank} \cdot C_{H_2O}} dt \quad (1)$$

$$Q_{reg}(t) = k_{H_2O} \cdot A_p \cdot (T_{reg}(t) - T_{chamber}(t)) \quad (2)$$

$T_{reg}(t)$ is the instant regeneration temperature that primarily affects the CCA's capture performance (K); $Q_w(t)$ is the instant collected useful thermal energy by ETC (W); $Q_{reg}(t-1)$ is the CCA's heat consumption at the former time step (t-1) (W) [18]; m_{water} is the water mass inside the thermal buffer tank (kg); k_{H_2O} is the heat transfer coefficient between the water and the adsorbent material (J/kg K); A_p is the contact area between water pipes and adsorbent particles (m²); $T_{chamber}(t)$ is the instantaneous temperature inside the chamber (K);

$$p_{CO_2}(t) = p_{CO_2}(t-1) + \frac{P_{atm} \cdot M_{air} \cdot \sum_1^4 d_{CO_2}^{j,k}(t)}{m_{room} \cdot M_{CO_2}} dt \quad (3)$$

$p_{CO_2}(t)$ is the instant indoor CO₂ partial pressure based on time-dependent calculation (Pa); $\dot{p}_{CO_2}(t)$ is the corresponding derived function (Pa/s); P_{atm} is the atmospheric pressure (Pa); M_{air} and M_{CO_2} are the molar mass of atmospheric air and CO₂ (g/mol), respectively; $\sum_1^4 d_{CO_2}^{j,k}(t)$ is the total increment of CO₂ mass, where k denotes 4 items: "new", "human", "cap", "back"; m_{room} is the total air mass inside the room (kg), which is a constant because of the restriction of mass balance, as shown below:

$$\sum_1^4 \dot{m}_{air}^{j,k}(t) = 0 \quad (4)$$

$$d_{CO_2}^{j,k}(t) = \frac{\dot{m}_{air}^{j,k}(t) \cdot M_{CO_2} \cdot C_{CO_2}^k(air)}{M_{air}} \quad (5)$$

$\dot{m}_{air}^{j,k}(t)$ are the instant mass flow rate of each gas stream (kg/s); $C_{CO_2}^k(air)$ is the CO₂ concentration of each gas stream k;

$$Q_{cool}^{conv}(t) = \dot{m}_{need}(t) \cdot C_{p(air)} \cdot (T_{amb}(t) - T_{room}) \quad (6)$$

$Q_{cool}^{conv}(t)$ is the cooling demand for conventional ventilation methods that can maintain the same plausible indoor CO₂ concentration level (<1000 ppm); $\dot{m}_{need}(t)$ is the accordingly mass flow rate of new-coming air from the outside (kg/s); $C_{p(air)}$ is the

specific heat capacity of ambient air (J/(kg K)); $T_{amb}(t)$ is the actual real-time ambient temperature data for 20 cities worldwide (K); T_{room} is the default room temperature, which is set as 297.15 K; T_{room} is also the adsorption temperature for the CCA device;

$$Q_{cool}^{now}(t) = \sum_k^{new,back} \dot{m}_{air}^{1 \text{ or } 3,1,k}(t_j) \cdot C_{p(air)} \cdot (T_{air}^{1 \text{ or } 3,1,k}(t) - T_{room}) \quad (7)$$

When the post-captured gas satisfies the temperature-concentration requirement of the electronic valve, air recirculation is valid (j=1), and the corresponding cooling demand of the proposed indoor air carbon capture system is calculated by Eq.(7). Two gas streams are included for j=1: new air supplied from the ambient and the recirculated "ideal gas" from CCA's adsorption process; The corresponding temperatures of these two gas streams are depicted by $T_{air}^{1,k}(t)$;

$$Q_{cool}^{now}(t) = \dot{m}_{air}^{1 \text{ or } 3,2,new}(t_j) \cdot C_{p(air)} \cdot (T_{amb}(t) - T_{room}) \quad (8)$$

When j=2, there is no recirculated air; thus, ambient air is the only inflow. And the proposed system's cooling demand is calculated by Eq. (8).

$$\beta = \frac{\int_{t_{min}}^{t_{max}} Q_{cool}^{conv}(t) dt - \int_{t_{min}}^{t_{max}} Q_{cool}^{now}(t) dt}{\int_{t_{min}}^{t_{max}} Q_{cool}^{conv}(t) dt} \times 100\% \quad (9)$$

β is the cooling energy-saving efficiency of the proposed system, which is calculated by the time-integrated items of instant cooling demand subject to both methods;

$$m_{CO_2} = \int_{t_{min}}^{t_{max}} (k_{CO_2} \times (m_{CO_2}^* - m_{CO_2}(t))) dt \quad (10)$$

$$m_{CO_2}^* = m_0(CO_2) \times \frac{KP_{CO_2}}{1 + KP_{CO_2}} \quad (11)$$

m_{CO_2} (kg) is the total collected CO₂ mass, based on the Linear Driven Force model [18, 19]; $m_{CO_2}^*$ is the intended equilibrium CO₂ mass result, which can be obtained by the Langmuir adsorption isotherm model as shown in Eq.(11); P_{CO_2} is the time-averaged indoor CO₂ partial pressure, which is also the partial pressure of the CCA device's feed gas.

3. RESULTS AND DISCUSSION

3.1 Time-dependent performance

After validating the subsystems with experimental references (excluded in this draft), Fig. 2 shows the time-dependent results of CO₂ uptakes and energy-saving performance of Phoenix, whose solar irradiance is also demonstrated in Fig. 2 (a). Black and green dashed lines show the cyclic CO₂ uptake amounts of chambers 1 and 2, which always work under alternative processes. The difference between the peak and valley point is the final collected CO₂ amount for each cycle. This value gets bigger when a higher regeneration temperature is achieved by higher solar irradiance. Fig. 2 (b) first compares the cooling demand of the conventional case (the top black line) and the proposed case (white shaded area). The difference between the two cases (E_{save}) is shaded in blue, 62.2 kWh/24 hours.

As mentioned in Fig. 1, an electronic valve is designed at the outlet of the adsorption chamber only to allow “ideal gas” to enter the

room. The red line depicts the temperature of returned air in Fig. 2 (b). The CO₂ concentration of returned air is always lower than ambient air, and that is why $\dot{m}_{air}^{1 \text{ or } 3,1,back}$ is always lower than \dot{m}_{need} ; thus, to decrease the cooling demand. The mass flow rates and temperatures of the corresponding air streams are marked in Fig. 2 (b). For each adsorption process, traveling air temperature always first increases from room temperature due to adsorption reaction. Once the outlet air temperature is higher than ambient temperature or its CO₂ concentration is higher than ambient conditions, the electronic valve turns off and stops the uncaptured gases from flowing back into the room. And this is when the gas stream from the ambient kicks in. As adsorption goes, the adsorbent gets saturated, and the reaction gets much milder; thus, the temperature goes down again and activates the electronic valve to allow air recirculation.

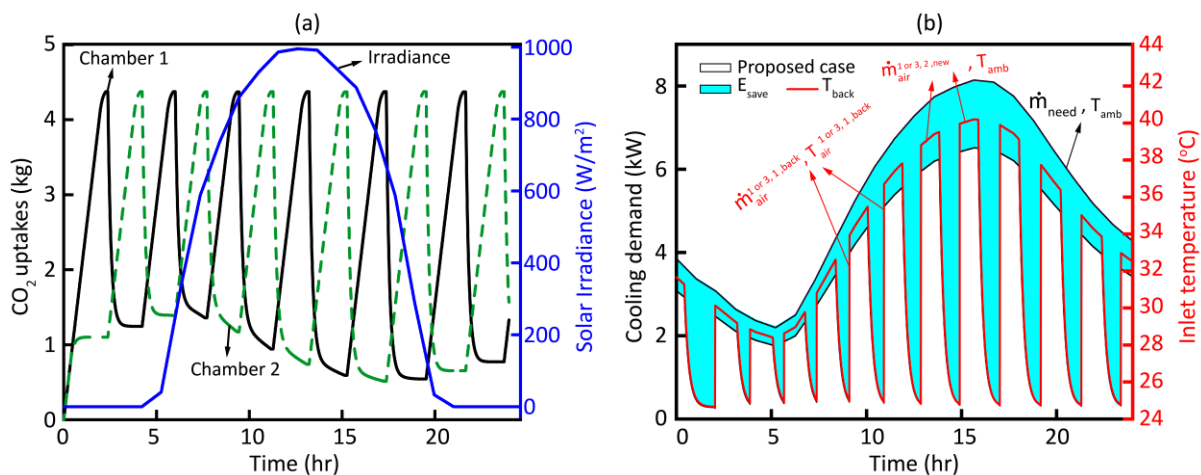


Fig. 2 Time-dependent analysis: (a) CO₂ uptake performance and solar irradiance; (b) Cooling demand

3.2 Global performance analysis

Fig. 3 is a holistic comparison of the hybrid systems’ cooling energy-saving performance and carbon capture performance. Specifically, Fig. 3 (a) uses different colors and circle radius to represent the magnitude of β . For example, yellow circles represent cities with a β value of between 38% and 43%, whereas the city name is shown at the bottom of the figure. A general

trend can be observed that both performances increase with the growing ambient temperature and solar irradiance. All the light purple circles fall in the “less hot” region, while all the highest-level circles fall in the “Very hot” area. The saved energy performance increases monotonically with increasing ambient temperature.

Notably, cities No.16 & 17, Yuma and Dakar, have a promising energy-saving performance of 47.28% and 46.79%, respectively, due to high ambient temperatures. However, due to low solar irradiance, according to Fig. 3 (b), they only capture 38.862 kg and 38.18 kg of CO₂ per day, which are lower than the amount of CO₂ exhaled by occupants (39.2 kg). In contrast, city No.15, Nagpur, achieves a β of 46.87% while still capturing 40.891 kg CO₂ per

day due to higher solar irradiance than cities No.16 & 17. Moreover, since the CCA device takes the indoor air as the feed gas, the ambient temperature doesn't directly influence the adsorbent's uptake ability. Instead, it is affected majorly by solar energy inputs. For example, in Fig. 3 (b), all the purple circles fall within the low sunlight zone, while all the blue circles fall within the "strong sunlight" zone.

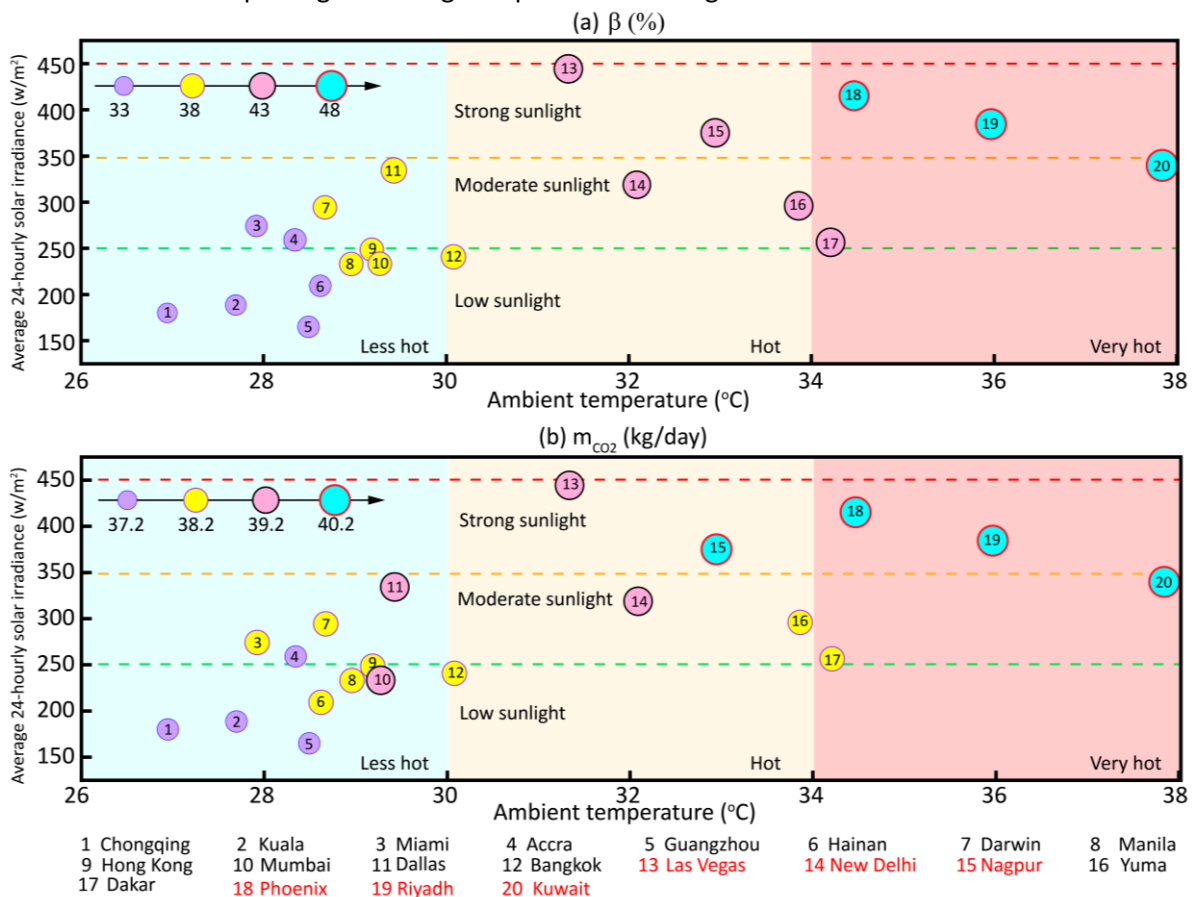


Fig. 3 Global performance analysis: (a) cooling energy-saving; (b) Collected CO₂ mass

4. CONCLUSION

This study uncovered the influence of solar irradiance, ambient temperature, and relative humidity on the novel system's carbon capture performance and cooling energy-saving performance. Specifically, a global analysis of weather conditions from 20 cities worldwide has been conducted on a solar-driven indoor air carbon capture system that considers real-time air recirculation. The main findings are enlisted below:

(1) For a 40 m² × 2.8 m with 39 occupants, the proposed system can capture 37.2 kg-41.03 kg CO₂ per day and achieves an energy

saving percentage of 23.95%-50.66% in different cities.

(2) Solar irradiance significantly affects the collected CO₂ mass, while the ambient temperature substantially affects the cooling energy-saving performance.

(3) Cities with rather high temperatures and strong solar irradiance perform better overall, such as Phoenix, Riyadh, and Kuwait. In contrast, less hot cities with low sun lights, such as Kuala and Miami, perform less ideally.

ACKNOWLEDGEMENT

The authors wish to acknowledge the financial support of the studentship provided by the Research Institute for Smart Energy (RISE) of The Hong Kong Polytechnic University.

REFERENCE

1. Pitarma, R., G. Marques, and B.R. Ferreira, *Monitoring Indoor Air Quality for Enhanced Occupational Health*. J Med Syst, 2017. **41**(2): p. 23.
2. agency, U.s.E.p., *What are the trends in indoor air quality and their effects on human health?*, U.s.E.p. agency, Editor. 2021.
3. Roberts, T., *We Spend 90% of Our Time Indoors. Says Who?*. 2016.
4. Mohammad Javad Jafari, A.A.K., Seyed Ali Mousavi Najarkola, Mir Saeed Yekaninejad, Mohammad Amin Pourhoseingholi, Leila Omid, Saba Kalantary, *Association of Sick Building Syndrome with Indoor Air parameters*. 2015.
5. CIBSE, *KS17: Indoor air quality & ventilation*, in *CIBSE knowledge series*. 2011, CIBSE.
6. VELUX. *Ventilation_Indoor air quality indicators*. Available from: <https://www.velux.com/what-we-do/research-and-knowledge/deic-basic-book/ventilation/indoor-air-quality?consent=preferences,statistics,marketing&ref-original=https%3A%2F%2Fwww.google.com%2F>.
7. Scheepers, P.T., et al., *Influence of a portable air treatment unit on health-related quality indicators of indoor air in a classroom*. J Environ Monit, 2012. **14**(2): p. 429-39.
8. *5 Ways to Improve Indoor Air Quality*. 2021; Available from: <https://www.co2meter.com/blogs/news/41775553-5-ways-to-improve-indoor-air-quality-in-your-home>.
9. *Indoor Air Quality*, O.S.a.H. Administration, Editor. 2021.
10. *Your Guide to Carbon Dioxide (CO2) Safety in the Workplace*. 2022.
11. KÜÇÜKHÜSEYİN, Ö., *CO₂ monitoring and indoor air quality*. REHVA Journal, 2021. **58**.
12. Satish, U., et al., *Is CO₂ an indoor pollutant? Direct effects of low-to-moderate CO₂ concentrations on human decision-making performance*. Environ Health Perspect, 2012. **120**(12): p. 1671-7.
13. Jacobson, T.A., et al., *Direct human health risks of increased atmospheric carbon dioxide*. Nature Sustainability, 2019. **2**(8): p. 691-701.
14. Kim, M.K., et al., *A novel ventilation strategy with CO₂ capture device and energy saving in buildings*. Energy and Buildings, 2015. **87**: p. 134-141.
15. Baus, L. and S. Nehr, *Potentials and limitations of direct air capturing in the built environment*. Building and Environment, 2022. **208**.
16. Harrouz, J.P., et al., *Feasibility of MOF-based carbon capture from indoor spaces as air revitalization system*. Energy and Buildings, 2022. **255**.
17. Wang, W., et al., *Efficient removal of CO₂ from indoor air using a polyethyleneimine-impregnated resin and its low-temperature regeneration*. Chemical Engineering Journal, 2020. **399**.
18. Shen, Y., T. Hocksun Kwan, and H. Yang, *Parametric and global seasonal analysis of a hybrid PV/T-CCA system for combined CO₂ capture and power generation*. Applied Energy, 2022. **311**.
19. Lei, M., *Thermal Swing Adsorption Process for Carbon Dioxide Capture and Recovery: Modeling, Simulation, Parameters Estimability, and Identification*. Industrial & Engineering Chemistry Research, 2013. **52**(22): p. 7526-7533.